BIOCHEMISTRY
including biophysical chemistry & molecular biology
Article

Biochemistry **2010,** *49,* 6617–6626 6617
DOI: 10.1021/bi100490u

Elucidation of the Functional Metal Binding Profile of a Cd^{II}/Pb^{II} Sensor $CmtR^{Sc}$ from *Streptomyces coelicolor*[†]

Yun Wang,[‡,⊥] John Kendall,[§] Jennifer S. Cavet,*[,§] and David P. Giedroc*[,‡,∥]

[‡]*Department of Biochemistry and Biophysics, Texas A&M University, College Station, Texas 77843-2128,* [§]*Faculty of Life Sciences, University of Manchester, Manchester, U.K., and* [∥]*Department of Chemistry, Indiana University, Bloomington, Indiana 47405-7102.* [⊥]*Present address: Division of Medicinal Chemistry, College of Pharmacy, The University of Texas, Austin, TX 78712.*

Received April 1, 2010; Revised Manuscript Received June 27, 2010

ABSTRACT: Metal homeostasis and resistance in bacteria is maintained by a panel of metal-sensing transcriptional regulators that collectively control transition metal availability and mediate resistance to heavy metal xenobiotics, including As^{III}, Cd^{II}, Pb^{II}, and Hg^{II}. The ArsR family constitutes a superfamily of metal sensors that appear to conform to the same winged helical, homodimeric fold, that collectively "sense" a wide array of beneficial metal ions and heavy metal pollutants. The genomes of many actinomycetes, including the soil dwelling bacterium *Streptomyces coelicolor* and the human pathogen *Mycobacterium tuberculosis*, encode over ten ArsR family regulators, most of unknown function. Here, we present the characterization of a homologue of *M. tuberculosis* CmtR ($CmtR^{Mtb}$) from *S. coelicolor*, denoted $CmtR^{Sc}$. We show that $CmtR^{Sc}$, in contrast to $CmtR^{Mtb}$, binds two monomer mol equivalents of Pb^{II} or Cd^{II} to form two pairs of sulfur-rich coordination complexes per dimer. Metal site 1 conforms exactly to the α4C site previously characterized in $CmtR^{Mtb}$ while metal site 2 is coordinated by a C-terminal vicinal thiolate pair, Cys110 and Cys111. Biological assays reveal that only Cd^{II} and, to a lesser extent, Pb^{II} mediate transcriptional derepression in the heterologous host *Mycobacterium smegmatis* in a way that requires metal site 1. In contrast, mutagenesis of metal site 2 ligands Cys110 or Cys111 significantly reduces Cd^{II} responsiveness, with no detectable effect on Pb^{II} sensing. The implications of these findings on the ability to predict metal specificity and function from metal-site signatures in the primary structure of ArsR family proteins are discussed.

The concentrations of first-row *d*-block transition metal ions and other heavier, toxic di- and trivalent metal ions and metalloids that play no biological role can vary dramatically in the immediate environment of a bacterial community. Although some are essential and enable proteins to adopt their native three-dimensional structures or function as cofactors for metalloenzyme catalysis, an excess beyond that required by normal cellular metabolism can also be strongly deleterious to cell viability (*1*). As a result, metal-specific regulatory systems have evolved that detect metal sufficiency or toxicity and control the intracellular availability of the different metal ions as well as purge any toxic elements or compounds from the cytosol. In free-living microorganisms, such detoxification/resistance systems are particularly important because they permit these organisms to survive by adaptation to potentially harsh environmental conditions, e.g., soil and water heavily contaminated by heavy metal salts (*2*) and/or the phagosome of mammalian host cells for certain microbial pathogens (*3*). Large, highly polarizable and thiophilic metal ions such as Hg^{II}, Cd^{II}, and Pb^{II} are highly toxic, in part because they are capable of forming high-affinity, kinetically long-lived complexes with protein cysteine thiolates found in native zinc binding sites, thereby rendering them nonfunctional. Such proteins include canonical zinc finger proteins and 5-aminolevulinic acid dehydratase (ALAD) in mammals (*4*, *5*).

CmtR is a Cd^{II}-sensing SmtB/ArsR (or ArsR) family metalloregulatory repressor from *Mycobacterium tuberculosis* (*6*−*9*). In addition to Cd^{II}, *M. tuberculosis* CmtR (denoted $CmtR^{Mtb}$ here) senses Pb^{II} in the heterologous host *Mycobacterium smegmatis* and has been shown to form Cys-thiolate-rich metal coordination complexes with Cd^{II}, Pb^{II}, and even Zn^{II} *in vitro* (*6*, *7*). CmtR possesses a unique pair of α4C metal binding sites (metal ligands derived from the α4 helix and the C-terminal tail; see Figure 1B) (*6*, *8*, *10*, *11*) structurally distinct from the Cd^{II}/Pb^{II} sites of another SmtB/ArsR Cd^{II}/Pb^{II} sensor, *Staphylococcus aureus* plasmid pI258-encoded CadC, which contains functional α3N and nonfunctional α5 metal sites (*1*, *12*, *13*). The solution structure of the CmtR−Cd^{II} complex reveals a homodimer with metal bound to Cys102′ from the C-terminal tail region of one subunit and Cys57, Cys61 in the helix α4 from the other subunit; Pb^{II} is predicted to bind to the same pair of sites (*7*, *8*) (Figure 1). Cys102 plays an accessory role in stabilizing the coordination complex while Cys57 and Cys61 anchor it, contributing most of the metal binding affinity (*7*). However, Cys102 does function as a key allosteric metal ligand in mediating the disassembly of oligomeric CmtR-*cmt* O/P[1] oligomeric complexes *in vitro* (*7*, *8*), and for derepression *in vivo* (*6*), although the structural and

[†]This work was supported, in whole or in part, by grants from the National Institutes of Health (GM042569 to D.P.G.) and the Biotechnology and Biological Sciences Research Council (BBSRC) (BB/G010765/1 to J.S.C.).

*To whom correspondence should be addressed. J.S.C.: tel, +44 161 275 51543; fax, +44 161 275 5082; e-mail, jennifer.s.cavet@manchester.ac.uk. D.P.G.: tel, 812-856-3178; fax, 812-856-5710; e-mail, giedroc@indiana.edu.

[1]Abbreviations: DTNB, 5,5′-dithiobis(2-nitrobenzoic acid); LMCT, ligand-to-metal charge transfer; O/P, operator/promoter.

Published on Web 06/29/2010

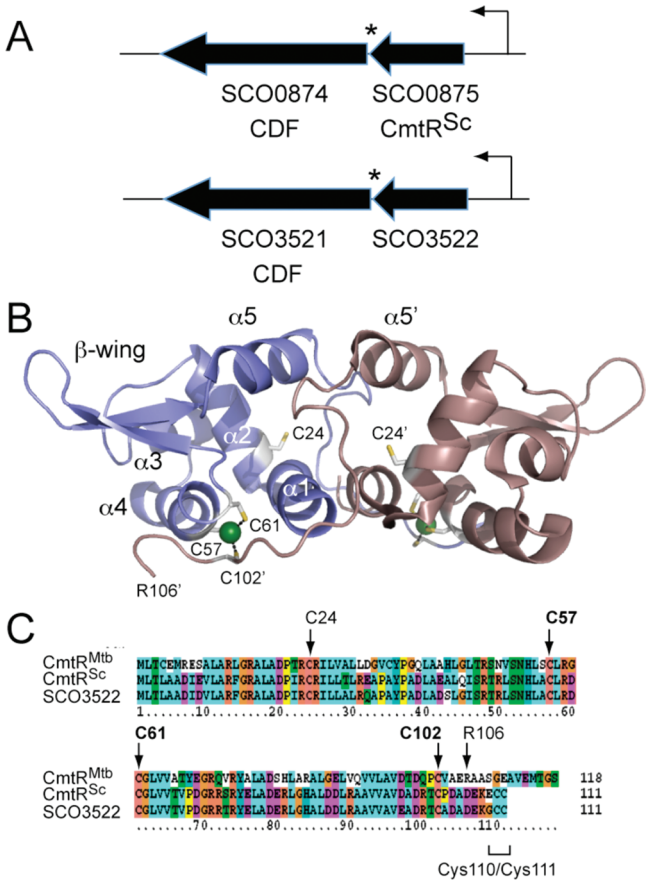

FIGURE 1: Genomic region of CmtR homologues in *S. coelicolor*, solution structure, and multiple sequence alignment of *M. tuberculosis* CmtR. (A) Genomic region around *S. coelicolor* CmtR^{Sc} (SCO0875) and SCO3522; each gene is separated by a single TGA termination codon (*) from homologous downstream genes SCO0874 and SCO3521 that encode putative CDF-family heavy metal transporters. The surrounding genomic regions are completely unrelated in the two loci. (B) Ribbon diagram of the solution structure of the *M. tuberculosis* CmtR−Cd^{II} complex (2jsc) with individual protomers shaded slate and violet and the two symmetry-related Cd^{II} ions colored green (*8*). The secondary structural units are labeled, with the side chains of C24 and the Cd^{II}-coordinating residues C57, C61, and C102′ (prime designation, opposite subunit) highlighted in stick. The most C-terminal residue in the structural model of each protomer is R106. (C) Multiple sequence alignment of CmtR^{Mtb}, CmtR^{Sc}, and the product of SCO3522. Cd^{II}-coordinating residues in CmtR^{Mtb} are highlighted in bold, with other residues as in panel B.

dynamic changes induced in the dimer upon Cys102 Cd^{II} binding remain to be characterized.

Recent *in vivo* experiments using *M. tuberculosis* suggest that CmtR^{Mtb} binds cooperatively to four binding sites in an extended 90-bp region upstream of the *cmtR-Rv1993c-cmtA* operon, to inhibit the interaction of RNA polymerase with the promoter region (*9*). These studies also suggest that Cd^{II} is the sole inducer in *M. tuberculosis*, a situation that contrasts with findings in the heterologous host, *M. smegmatis* (*6*, *9*). The *cmtA* gene encodes a deduced metal transporting P_{1B}-ATPase efflux pump, which is proposed to efflux toxic metal ions from the bacterial cytosol (*6*, *9*). Therefore, increasing cellular Cd^{II} concentration triggers derepression of the *cmtR-Rv1993c-cmtA* operon, resulting in increased concentrations of CmtA in the plasma membrane which is thought to export Cd^{II} from the cytosol against a metal concentration gradient (*9*).

Streptomyces coelicolor A3(2) is representative of a ubiquitous group of soil-dwelling, filamentous Gram-positive bacteria. This highly adaptable organism undergoes a broad range of metabolic processes and biotransformations and is noted for its natural antibiotic production (*14*). Like *M. tuberculosis*, *S. coelicolor* belongs to the taxonomy order of *Actinomycetales* (*14*, *15*). Although each has very different lifestyles, both encode elaborate metal detoxification and efflux systems. As a human pathogen, *M. tuberculosis* must adapt to various microenvironmental niches, including the phagosome of infected macrophages where it likely encounters changes in metal availability (*3*, *16*−*19*). *S. coelicolor* must also sense and respond to fluctuating metal levels within soils (*20*−*22*). Notably, the sequenced strains of *M. tuberculosis* and *S. coelicolor* possess multiple deduced ArsR family regulators, ten (*10*) and fourteen, respectively, as well as representatives of many of the other metalloregulatory protein classes (*1*, *23*). The diversity of the metal-responsive regulators in these two organisms is therefore likely to reflect their different ecological niches and the different survival strategies employed to avoid metal stress. A search for protein homologues of *M. tuberculosis* CmtR returned two open reading frames in *S. coelicolor* A3(2) corresponding to locus tags SCO0875 and SCO3522. The gene products of SCO0875 and SCO3522 possess only ten amino acid differences between them, and each shares ≈50% identity with *M. tuberculosis* CmtR. Both SCO0875 and SCO3522 are immediately upstream of deduced cation diffusion facilitator (CDF) family integral membrane metal transporters (Figure 1A), with predicted roles in the transport of the more thiophilic metal ions (*24*). SCO0875 was chosen for detailed study herein and designated CmtR^{Sc}.

CmtR^{Sc} shares four conserved cysteine residues with CmtR^{Mtb} which include the three Cd^{II} ligands (Cys57, Cys61, and Cys102) required for metal binding and allosteric regulation (*6*) as well as C24 in the α2 helix (Figure 1A). As a result, we expected to observe at least partially similar metal binding profiles for CmtR^{Mtb} and CmtR^{Sc}. However, CmtR^{Sc} contains two additional cysteines arranged as a C-terminal vicinal pair (Cys110 and Cys111) that could also be involved in metal coordination (Figure 1C). It was therefore of interest to functionally and structurally characterize CmtR^{Sc} and compare its properties to that of CmtR^{Mtb}. We show here that the CmtR^{Sc} homodimer harbors a second pair of high-affinity Cys-thiolate-rich Cd^{II}/Pb^{II} coordination sites relative to CmtR^{Mtb} that involves metal coordination by Cys110 and Cys111. We further show that wild-type CmtR^{Sc} is a *bona fide* CmtR that is highly selective for Cd^{II}/Pb^{II} in the heterologous host *M. smegmatis*, the same host used to characterize CmtR^{Mtb}, with no other metal ions, including Hg^{II} and Zn^{II}, capable of inducing transcriptional derepression. Strikingly, the second pair of Cd^{II}/Pb^{II} sites unique to CmtR^{Sc} is required for full Cd^{II} responsiveness in *M. smegmatis* but does not alter Pb^{II} sensing under the same conditions. The structural and functional implications of these findings for the prediction of metal-sensing sites in ArsR family metal sensors are discussed.

MATERIALS AND METHODS

Construction of Wild-Type and C110G/C111S CmtR^{Sc} Overexpression Plasmids. To create pET3a-CmtR^{Sc}, the CmtR^{Sc} coding region was amplified by PCR from *Streptomyces violaceoruber* genomic DNA (M145, used in to sequence the *S. coelicolor* genome (*14*) using primers V (5′-AAAAACATATGGTGCTGACTCTCGCTGCCGATATC-3′) and VI (5′-AAAAAGCTAAGCTCAGCAGCACTCCTTCTCGTC-3′) and cloned into

pET3a (Novagen) between the *Nde*I and *BPU1102*I restriction sites using standard methods. The plasmid encoding C110G/C111S CmtR^{Sc} was generated by site-directed mutagenesis using the QuikChange kit (Stratagene) and primers VII (5′-GGACGAGAAGGAGGGCTCCTGAGCAATAACTAGC-3′) and VIII (5′-GCTAGTTATTGCTCAGGAGCCCTCCTTCTCGTCC-3′) using pET3a-CmtR^{Sc} as the template. The integrity of all expression plasmids was verified by DNA sequencing.

Purification of Wild-Type and Mutant CmtR^{Sc}. CmtR^{Sc} and C110G/C111S CmtR^{Sc} were purified to homogeneity using a procedure previously described for CmtR^{Mtb} (*7*). The theoretical molecular mass for CmtR^{Sc} is 12.2 kDa, and the extinction coefficient was calculated to be 3730 $M^{-1}\cdot cm^{-1}$.

Free Thiol Determination. A standard DTNB[1] colorimetric assay was used to determine the number of free thiols in CmtR^{Sc} (*25*). Twenty-five microliters of 2.5 mM DTNB solution was added separately into 400 μL of 10−15 μM protein. After a 30 min incubation in the anaerobic chamber, the concentration of thiolate anion was quantified at 412 nm (ε = 13600 $M^{-1}\cdot cm^{-1}$) after subtraction of the absorbance of the final dialysis buffer with the same concentration of DTNB. The number of free thiols in wild-type CmtR^{Sc} was 5.8 ± 0.2 (6 expected) and 3.0 ± 0.2 (4 expected) for C110G/C111S CmtR^{Sc}.

Atomic Absorption Spectroscopy. The concentrations of all metal titrants were determined using a Perkin-Elmer Analyst 700 atomic absorption spectrophotometer operating in flame mode using different hollow cathode lamps specific for each metal (*25*). Zn^{II} was detected at 213.9 nm (slit = 0.7 nm), Cd^{II} was detected at 228.8 nm (slit = 0.7 nm), and Pb^{II} was detected at 283.3 nm (slit = 0.7 nm).

Analytical Sedimentation Equilibrium Ultracentrifugation. All experiments were carried out on a Beckman Optima XL-A analytical ultracentrifuge with the rotor speed set to 20000 rpm at 25.0 °C. Ultracentrifuge cells were assembled in the anaerobic glovebox and contained 5.0 μM CmtR^{Sc} wild type or 8.0 μM C110G/C111S CmtR^{Sc} in buffer (10 mM Hepes, 0.4 M NaCl, and 0.1 mM EDTA at pH 7.0). Scans were monitored by absorbance at 232 or 233 nm for the wild-type and C110G/C111S CmtR^{Sc}, respectively, with the final seven scans extracted and subjected to simultaneous fitting using Ultrascan II 8.0. A partial specific volume (ν) of 0.7354 mL/g (predicted by Sednterp 1.07 software, www.bbri.org/RASMB/rasmb.html) and a buffer density (ρ) of 1.0 g/mL were used in the analysis. The data were globally and simultaneously fitted to either a one-component ideal species model or a monomer−dimer equilibrium model using eqs 1 and 2, respectively:

$$C(X) = e^{[\ln(A)+M\omega^2(1-\overline{\nu}\rho)(X^2-X_r^2)]/2RT} + B \quad (1)$$

$$C(X) = e^{[2\ln(A)+\ln(2/EL)+\ln(K_{1,2})+2M\omega^2(1-\overline{\nu}\rho)(X^2-X_r^2)]/2RT} + e^{[\ln(A)+M\omega^2(1-\overline{\nu}\rho)(X^2-X_r^2)]/2RT} + B \quad (2)$$

where X = cell radius, X_r = reference radius, A = amplitude of monomer*, M = molecular weight of monomer*, E = extinction coefficient, R = gas constant, T = temperature, B = baseline offset*, ω = angular velocity, L = optical path length, $K_{1,2}$ = monomer−dimer equilibrium constant*, and * indicates this parameter can be floated during parameter optimization (*26*). Fits to the monomer−dimer model did not significantly improve the goodness of fit, consistent with a low concentration of monomeric species under these solution conditions; thus, $K_{1,2} \geq 10^6$ M^{-1}.

Cd^{II}, Pb^{II} Optical Absorption Spectroscopy. All metal binding experiments were carried out anaerobically at ambient temperature (~25 °C) using a Hewlett-Packard model 8452A spectrophotometer (*12*, *27*). For Cd^{II} titrations, apoproteins were diluted using final dialysis buffer S to ≈50 μM in 800 μL and loaded into an anaerobic cuvette fitted with a Hamilton gastight adjustable volume syringe containing 0.5 mM Cd^{II} titrant in the glovebox. Complete optical spectra of apoprotein were collected from 200 to 900 nm 1−2 min after each addition of a known aliquot (5−15 μL) of Cd^{II}. Corrected spectra were obtained by subtraction of the apoprotein spectra from each spectrum obtained after addition of metal ion and further corrected for dilution. Pb^{II} titrations were done in exactly the same way except that 10 mM Bis-Tris and 0.4 M NaCl, pH 7.0, was used as the buffer. Bis-Tris is a weakly chelating buffer that can prevent excess Pb^{II} from forming $Pb^{II}(OH)_2$ precipitate (*4*). Cd^{II} competition experiment performed with EDTA was carried out as described above except 200−300 μM chelator was present. The competition binding curves were fit to the model using Dynafit:

$$P + Cd \leftrightarrows P\cdot Cd \quad K_{Cd1}$$

$$P\cdot Cd + Cd \leftrightarrows P\cdot Cd2 \quad K_{Cd2}$$

$$EDTA + Cd \leftrightarrows EDTA\cdot Cd \quad K_{Cd\text{-}EDTA}$$

where P is the monomer concentration of CmtR^{Sc} and $K_{Cd\text{-}EDTA}$ (pH 7.0) = 8.31×10^{13} M^{-1} under these conditions using a pH-dependent log K_{Cd} = 16.5 and pK_as of 9.52 and 6.13 for EDTA (*28*).

Zn^{II} Binding Experiments. The zinc chelator dye magfura-2 (K_{Zn} = 5.0×10^7 M^{-1} at pH 7.0 and 25 °C) was used as a colorimetric competitor for Zn^{II} binding by wild-type and C110G/C111S CmtR^{Sc} as previously described (*29*). Thirty micromolar CmtR^{Sc} and ≈15 μM magfura-2 were used for all experiments. The data were fit to a competitive binding model assuming two nonequivalent, noninteracting metal binding sites per CmtR^{Sc} protomer for CmtR^{Sc} wild type by DynaFit:

$$P + Zn \leftrightarrows P-Zn \quad K_{PZn}$$

$$P\cdot Zn + Zn \leftrightarrows P-Zn_2 \quad K_{PZn2}$$

$$magfura\text{-}2 + Zn \leftrightarrows magfura\text{-}2-Zn$$

where $K_{Zn-magfura\text{-}2}$ = 5.0×10^7 M^{-1} under these conditions. For C110G/C111S CmtR^{Sc}, data were fitted as above to a competitive binding model assuming one metal binding site per protomer or two per dimer (without K_{PZn2}).

Construction of Promoter−lacZ Fusions, Site-Directed Mutagenesis, and β-Galactosidase Assays. CmtR^{Sc} upstream sequences and the coding region (539 bp) were amplified from *S. coelicolor* genomic DNA using primers 5′-GAAAGTACTGCGGGTAGTGGCGATGTGATCC-3′ and 5′-GAAGGTACCGCGGTCATTCAGCAGC-3′ and ligated to pGEM-T prior to subcloning into the *Sca*I/*Kpn*I site of pJEM15 (*30*) to create a transcriptional fusion with *lacZ*. QuickChange XL (Stratagene) site-directed mutagenesis was subsequently employed to generate derivatives with the following codon substitutions in CmtR^{Sc}: Cys24, Cys57, Cys61, Cys102, Cys110, and Cys111, each to Ser; and Arg16 to a UGA stop codon. All generated plasmid constructs were checked by sequence analysis. *M. smegmatis* mc^{2}155 was used as an actinomycete host for reporter gene assays.

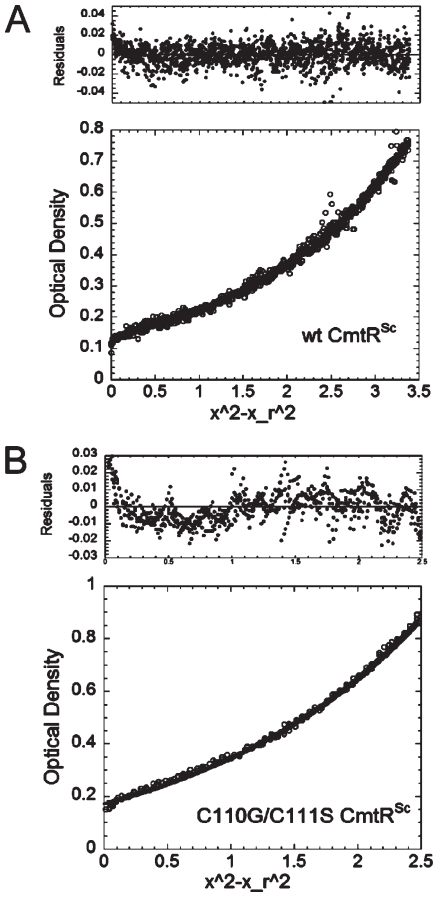

FIGURE 2: Analytical sedimentation equilibrium ultracentrifugation of $CmtR^{Sc}$ and C110G/C111S $CmtR^{Sc}$. (A) 5.0 μM monomer wild-type $CmtR^{Sc}$. (B) 8.0 μM monomer C110G/C111S $CmtR^{Sc}$. Filled symbols in upper panels represent an overlay of data collected during the last seven scans and indicate that equilibrium had been reached. The solid line represents the global simultaneous fit for a single ideal species model using Ultrascan. For wild-type $CmtR^{Sc}$, the fitted M_w is 23820 Da (theoretical dimer M_w = 24378 Da), variance = 1.0689 e^{-4}. For C110G/C111S $CmtR^{Sc}$, the fitted M_w is 25690 Da (theoretical dimer M_w = 24252 Da), variance = 5.8026 e^{-5}. Conditions: 10 mM Hepes, 0.4 M NaCl, and 0.1 mM EDTA at pH 7.0, 25.0 °C, and 20000 rpm rotor speed.

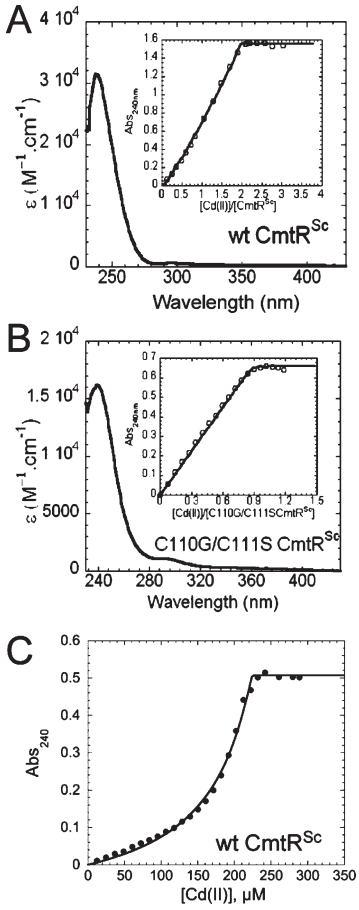

FIGURE 3: Cd^{II} titrations of wild-type and C110G/C111S $CmtR^{Sc}$. (A) Apoprotein-subtracted difference spectrum of wild-type $CmtR^{Sc}$ (50.7 μM monomer). (B) Apoprotein-subtracted difference spectrum of C110G/C111S $CmtR^{Sc}$ (44.8 μM monomer). $CmtR^{Sc}$ variants were titrated anaerobically with increasing concentrations of Cd^{II}. Inset: Cd^{II} binding isotherm plotted as change in A_{240} vs [$CmtR^{Sc}$ variant monomer]. (C) Cd^{II}-EDTA competition binding isotherm in which 20.9 μM wild-type $CmtR^{Sc}$ was titrated with Cd^{II} in the presence of 227 μM EDTA. Conditions: 10 mM Hepes, 0.4 M NaCl, pH 7.0, 25 °C.

The *lacZ* fusion constructs were introduced into *M. smegmatis* and transformants selected on Luria−Bertani (LB) agar supplemented with 25 μg mL^{-1} kanamycin as described previously (*30*). β-Galactosidase assays were performed as described (*31*) in triplicate on at least three separate occasions. Cells were grown at 37 °C with shaking in LB broth or Sauton medium containing 0.05% (v/v) Tween 80 and kanamycin (25 μg mL^{-1}) supplemented with the indicated concentration of metal salt (described in individual experiments) for ~20 h immediately prior to assays. The metal salts used were $ZnSO_4$, $CoSO_4$, $NiCl_2$, $CdCl_2$, $Pb(C_2H_3O_2)_2$, $CuSO_4$, $AsNaO_2$, and $HgCl_2$.

RESULTS

Wild-Type and C110G/C111S $CmtR^{Sc}$ Are Stable Homodimers at Low Protein Concentrations. Both $CmtR^{Sc}$ and its C110G/C111S mutant were subjected to analytical equilibrium sedimentation ultracentrifugation at 20000 rpm at 5 and 8 μM monomer concentration, respectively, and absorbance was recorded at 232 nm, with representative results shown in Figure 2. Each set of experimental data that had reached equilibrium was first subjected to a global simultaneous fit to a single ideal species model indicated by a solid line. The apparent molecular weights obtained from these data (Figure 2) are consistent with both apo-$CmtR^{Sc}$ and apo-C110G/C111S $CmtR^{Sc}$ being predominantly homodimeric under these conditions.

$CmtR^{Sc}$ Possesses Two Cd^{II} Binding Sites per Monomer While C110G/C111S $CmtR^{Sc}$ Possesses One. Apoprotein-subtracted Cd^{II} absorbance spectra of $CmtR^{Sc}$ are shown in Figure 3. The saturated Cd^{II} spectra are characterized by an intense ligand-to-metal charge transfer (LMCT)[1] at 240 nm, similar to that observed for $CmtR^{Mtb}$ (*7*). Binding isotherms (insets) were obtained by plotting the corrected absorbance at 240 nm as a function of total [Cd^{II}] over protein monomer ratio. The maximum molar absorptivity at 240 nm for $CmtR^{Sc}$ is ≈31000 $M(monomer)^{-1}$ cm^{-1}, which is 2-fold larger than wild-type mycobacterial $CmtR^{Mtb}$ ($\varepsilon \approx 16000$ M^{-1} cm^{-1}) (Figure 3A) (*7*). In addition, $CmtR^{Sc}$ exhibits a 2:1 (Cd^{II}:$CmtR^{Sc}$ monomer) binding stoichiometry (Figure 3A), in contrast to $CmtR^{Mtb}$ which is known to bind one metal per protomer (*7*). Nonlinear least-squares fits of the binding isotherms to a simple 2:1 independent-site metal binding model return only a lower limit of the binding affinity given the stoichiometric nature of these binding curves ($K_{Cd} > \approx 5 \times 10^7$ M^{-1}) (Figure 3A).

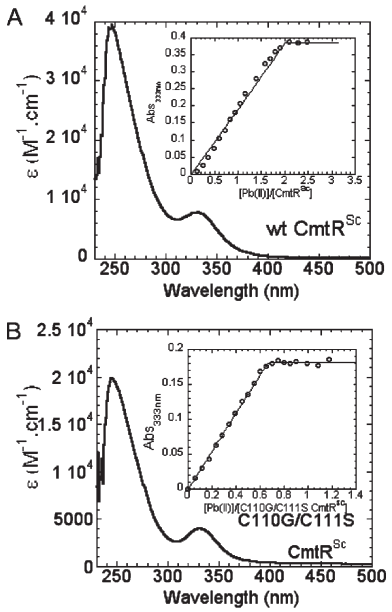

FIGURE 4: Pb^{II} titrations of $CmtR^{Sc}$ and C110G/C111S $CmtR^{Sc}$. (A) Apoprotein-subtracted difference spectrum of wild-type $CmtR^{Sc}$ (50.8 μM). (B) Apoprotein-subtracted difference spectrum of C110G/C111S $CmtR^{Sc}$ (53.7 μM). $CmtR^{Sc}$ variants were titrated anaerobically with increasing concentrations of Pb^{II}. Inset: Pb^{II} binding isotherm plotted as change in A_{333} vs [$CmtR^{Sc}$ variant monomer]. Conditions: 10 mM Bis-Tris, 0.4 M NaCl, pH 7.0, 25.0 °C.

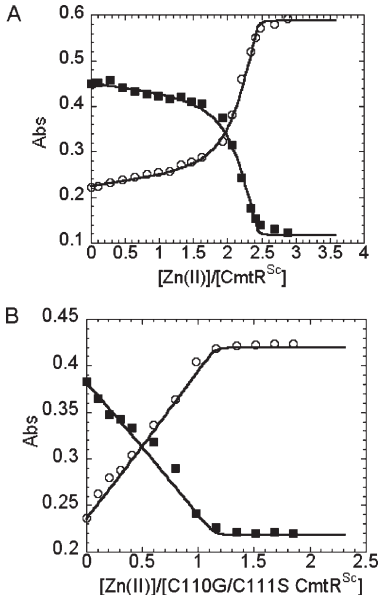

FIGURE 5: Zn^{II} titrations of $CmtR^{Sc}$ and C110G/C111S $CmtR^{Sc}$ using magfura-2 as an indicator. (A) 30 μM $CmtR^{Sc}$ and 14.7 μM magfura-2 and (B) 30 μM C110G/C111S $CmtR^{Sc}$ and 15 μM magfura-2 were present. The empty circles represent A_{325} ,and the filled squares represent A_{366}. The solid line represents a global nonlinear least-squares fit to a model that incorporates the stepwise binding of two Zn^{II} (defined by K_{PZn} and K_{PZn2}) to a $CmtR^{Sc}$ monomer using Dynafit. The titration for C110G/C111S $CmtR^{Sc}$ was fitted using one Zn^{II} to protein monomer binding model. The following parameters were obtained for wild-type $CmtR^{Sc}$: $K_{PZn} = 5.3\ (\pm 1.8) \times 10^8\ M^{-1}$ (a lower limit under these conditions), $K_{PZn2} = 6.7\ (\pm 1.4) \times 10^8\ M^{-1}$. For C110G/C111S $CmtR^{Sc}$, $K_{PZn} = 5.5\ (\pm 1.2) \times 10^7\ M^{-1}$. Conditions: 10 mM Hepes, 0.4 M NaCl at pH 7.0 and 25.0 °C.

The presence of an additional Cd^{II} site in the $CmtR^{Sc}$ homodimer coupled with twice the Cys $S^- \rightarrow Cd^{II}$ molar absorptivity prompted us to investigate if the two vicinal cysteine residues (Cys110 and Cys111) at the C-terminus donate thiolate ligands to the second Cd^{II} ion. We measured the Cd^{II} absorption spectrum of C110G/C111S $CmtR^{Sc}$, where the two C-terminal cysteines were converted to their analogous residues in $CmtR^{Mtb}$ (Figure 1C). As expected, C110G/C111S $CmtR^{Sc}$ behaves much like $CmtR^{Mtb}$, given an ≈0.9:1 Cd^{II}:C110G/C111S monomer stoichiometry and an identical monomer molar absorptivity of ≈16000 M^{-1} cm^{-1} (Figure 3B) (*7*), which is precisely half that of wild-type $CmtR^{Sc}$. As expected, the binding of Cd^{II} is stoichiometric under these conditions and thus returns only a lower limit of the metal binding affinity (Figure 3B). Given a molar absorptivity of ≈5500 M^{-1} cm^{-1} per Cd−S coordination bond (*32*−*34*), it is reasonable to conclude that C110G/C111S $CmtR^{Sc}$ possesses one Cd^{II} site (termed metal site 1) that is identical to the previously characterized canonical α4C site $CmtR^{Mtb}$, while wild-type $CmtR^{Sc}$ possesses two spectroscopically similar Cd^{II} binding sites (metal sites 1 and 2).

The Cd^{II} affinities of each metal site per monomer in wild-type $CmtR^{Sc}$ were estimated by carrying out a Cd^{II} titration experiment in the presence of a known concentration of the metal chelator EDTA (Figure 3C), with $K_{Cd\text{-}EDTA} = 8.3 \times 10^{13}\ M^{-1}$ under these solution conditions (pH 7.0, 25.0 °C). A nonlinear least-squares fit of a simple competition model assuming two nonequivalent, noninteracting sites per protomer gives $K_{Cd1} = 3.0\ (\pm 0.1) \times 10^{13}\ M^{-1}$, $K_{Cd2} = 3.6\ (\pm 0.5) \times 10^{12}\ M^{-1}$. These data taken together confirm that $CmtR^{Sc}$ has two pairs of structurally similar high-affinity metal sites per homodimer, which differ in macroscopic affinity by ≈10-fold. Previous findings with $CmtR^{Mtb}$ reveal that Cys57, Cys61, and Cys102 are ligands to Cd^{II} and form trigonal pyramidal coordination geometry (S_3) or distorted tetrahedral coordination geometries (S_3O), with Cys102 not as strongly bound as the other thiolate ligands (*6*−*8*) (see Figure 1B). Considering these three cysteines are conserved in $CmtR^{Mtb}$ and $CmtR^{Sc}$, they likely create a Cd^{II} site indistinguishable to that in $CmtR^{Mtb}$ and are denoted metal site 1. In contrast, Cd^{II} site 2 clearly requires coordination by Cys110 and Cys111.

$CmtR^{Sc}$ Possesses Two Pb^{II} Binding Sites, and the Same C110G/C111S Mutation Abolishes One. Anaerobic Pb^{II} titration experiments were performed using ≈50 μM apo-wild-type $CmtR^{Sc}$ (Figure 4A) and C110G/C111S $CmtR^{Sc}$ (Figure 4B), and the apoprotein-subtracted difference spectra are shown. The saturated Pb^{II} spectra of both proteins are characterized by an intense absorption in the far-ultraviolet and a long-wavelength absorption band with maximum at 333 nm, identical to that of $CmtR^{Mtb}$ (*7*), and report on ligand-to-metal charge transfer (S^- 3p → Pb 6p) and intraatomic (Pb $6s^2$ → Pb 6sp) electronic transitions (*35*, *36*). Binding isotherms (insets) were obtained by plotting the corrected absorbance at 333 nm as a function of total [Pb^{II}]/protein monomer ratio. As expected, for wild-type $CmtR^{Sc}$ Pb^{II} binding is saturable at ≈2:1 ratio over [$CmtR^{Sc}$] monomer (Figure 4A); in contrast, this stoichiometry drops to ≈0.7 Pb^{II}/monomer for C110G/C111S $CmtR^{Sc}$ (Figure 4B). These Pb^{II} stoichiometries are largely consistent with the relative monomer molar absorptivities at 333 nm (ε_{333}) of ≈7900 M^{-1} cm^{-1} and ≈3950 M^{-1} cm^{-1} for wild-type $CmtR^{Sc}$ and C110G/C111S $CmtR^{Sc}$, respectively (Figure 4). Interestingly, the Pb^{II}-thiolate molar absorptivity of C110G/C111S $CmtR^{Sc}$ appears to be about one-half that of $CmtR^{Mtb}$ (*7*) for reasons that are not clear, although the fractional stoichiometries in each case may complicate this. Furthermore, the extent to which molar absorption wavelength and intensity reports on coordination number and

geometry for Pb^{II}-thiolate complexes has not yet been firmly established, unlike for other metal ions (*12*, *36*−*39*). In any case, the simplest conclusion is that substitution of Cys110 and Cys111 with nonliganding residues abolishes Pb^{II} binding to metal site 2, as is the case for Cd^{II}.

$CmtR^{Sc}$ Binds Two Zn^{II} per Monomer As Determined by Chelator Competition Experiments with Magfura-2. The zinc indicator dye magfura-2 ($K_{Zn\cdot magfura\text{-}2} = 5.0 \times 10^7\ M^{-1}$) was used as a competitor of Zn^{II} binding to $CmtR^{Sc}$ and the C110G/C111S mutant to determine the Zn^{II} binding stoichiometry and affinity constant K_{Zn} (*11*). Figure 5 shows representative titrations of Zn^{II} into mixtures of wild-type $CmtR^{Sc}$ (Figure 5A) and C110G/C111S $CmtR^{Sc}$ (Figure 5B) and magfura-2. The solid curve represents a fit to a model that describes the binding of two Zn^{II} ions to the wild-type $CmtR^{Sc}$ monomer, again considering each monomer−metal binding as an independent event (Figure 5A). For wild-type $CmtR^{Sc}$, the estimated parameters are similar for both zinc ions, with $K_{PZn} = 5.3\ (\pm 1.8) \times 10^8\ M^{-1}$ and $K_{PZn2} = 6.7\ (\pm 1.4) \times 10^8\ M^{-1}$. These binding affinities differ from that determined previously for the $CmtR^{Mtb}$ dimer, which showed strong negative cooperativity within the dimer with one site in $\approx 10^{10}\ M^{-1}$ range and the other in $\sim 10^5\ M^{-1}$ range under the same solution conditions (*7*). For the C110G/C111S $CmtR^{Sc}$ mutant, competition titration curves were fit to a model that describes the binding of one Zn^{II} ion to the C110G/C111S $CmtR^{Sc}$ monomer (Figure 5B), with an estimated affinity of $K_{PZn} = 5.5\ (\pm 1.2) \times 10^7\ M^{-1}$.

Cadmium and Lead Alleviate $CmtR^{Sc}$-Mediated Repression. *M. smegmatis* mc^2155 was previously used to characterize $CmtR^{Mtb}$ and hence was exploited as a heterologous host for the characterization of $CmtR^{Sc}$, thereby allowing direct comparison of these two regulators within the same cytosol. *M. smegmatis* mc^2155 and *S. coelicolor* are closely related actinomycetes, with similarly high GC contents, and recognition of *Streptomyces* operator−promoter elements by the mycobacterial transcription machinery (*40*, *41*) has been exploited previously to characterize *S. coelicolor* genes *in vivo* (*41*). To determine which, if any, metals are sensed by $CmtR^{Sc}$ *in vivo*, a 539-bp DNA fragment including the *$cmtR^{Sc}$* operator−promoter and coding region was fused to a promoterless *lacZ* in plasmid pJEM15 and introduced into *M. smegmatis* mc^2155. β-Galactosidase activity was measured following growth (~20 h) of cells in medium supplemented with maximum permissive concentrations of various metals. At these biologically significant metal levels, elevated activity was detected in response to Cd^{II} and, to a lesser extent, Pb^{II} but no other metals (Figure 6A). Furthermore, in the absence of added metal ions, elevated β-galactosidase activity was detected in cells containing an analogous construct in which codon 16 within the *$cmtR^{Sc}$* coding region was converted to a stop codon (Figure 6B), confirming that $CmtR^{Sc}$ acts negatively toward expression.

$CmtR^{Sc}$ Senses Cd^{II} and Pb^{II} Using α4C Sites. The previously characterized Cd^{II} binding α4C sensing sites of $CmtR^{Mtb}$ involve Cys102 from the C-terminal region of one subunit in association with Cys57 and Cys61 from helix αR of the other subunit (*6*−*8*) (see Figure 1B). Comparison of the amino acid sequences of $CmtR^{Sc}$ and related ArsR family sensors reveals that the α4C ligands are completely conserved in $CmtR^{Sc}$ and $CmtR^{Mtb}$, while $CmtR^{Sc}$ lacks residues corresponding to other previously defined ArsR family metal binding motifs (*1*, *10*). Substitution of the α4C cysteines (Cys57, Cys61, and Cys102) in $CmtR^{Sc}$ with serines created functional repressors that mediated low expression of *lacZ* in cells grown with no metal supplement,

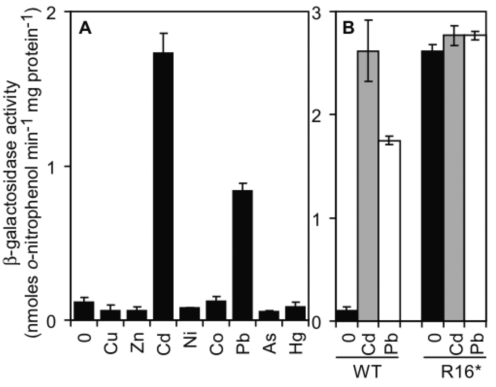

FIGURE 6: $CmtR^{Sc}$ responds to Cd^{II} and Pb^{II} in an actinomycete host. (A) β-Galactosidase activity measured in *M. smegmatis* mc^2155 containing *$cmtR^{Sc}$* and its operator-promoter region fused to *lacZ* following growth in LB medium with no metal supplement or with maximum permissive concentrations of Zn^{II} (100 μM), Co^{II} (200 μM), Ni^{II} (500 μM), Cd^{II} (7.5 μM), Cu^{II} (500 μM), Pb^{II} (3.75 μM), As^{III}(20 μM), or Hg^{II} (0.025 μM). (B) β-Galactosidase activity in cells containing wild-type $CmtR^{Sc}$ (WT) or the stop codon derivative (R16*) following growth in LB medium with no metal supplement (black) or maximum permissive concentrations of Cd^{II} (gray) or Pb^{II} (white).

but repression was not alleviated at Cd^{II} concentrations that caused loss of repression by wild-type $CmtR^{Sc}$ (Figure 7A). In addition, no alleviation of repression was observed in the presence of maximum permissive concentrations of Pb^{II} (Figure 7A). Hence, consistent with findings for $CmtR^{Mtb}$ (*6*), Cys57, Cys61, and Cys102 at α4C are obligatory for both Cd^{II} and Pb^{II} recognition by $CmtR^{Sc}$ *in vivo* and likely contribute toward a single common metal binding site, metal site 1.

Cd^{II}, but Not Pb^{II}, Sensing by $CmtR^{Sc}$ Involves an Additional Pair of C-Terminal Cysteines. As discussed above, in addition to Cys57, Cys61, and Cys102 at α4C, $CmtR^{Sc}$ possesses three further cysteines (Cys24 found in both CmtRs and Cys110 and Cys111 which are unique to $CmtR^{Sc}$, Figure 1C). In the absence of added Cd^{II} or Pb^{II}, β-galactosidase activity remained low in cells containing Ser substitutions of Cys24, Cys110, or Cys111, consistent with retention of repressor function (Figure 7A). However, although inducer recognition was clearly retained in these cells, Cd^{II}-mediated derepression was substantially reduced in cells containing the single Cys110 and Cys111 substitution mutants (Figure 7A). Indeed, when expression from the *cmtR* operator−promoter was examined in cells exposed to a range of Cd^{II} and Pb^{II} concentrations, Cd^{II} responsiveness was significantly impaired for the C110S and C111S mutants at all cadmium concentrations up to inhibitory levels, whereas Pb^{II} responsiveness appeared unaffected (Figure 7B). Equivalent findings were also obtained using minimal (Sauton) medium (Figure 8) which reveals no significant reduction in the magnitude of derepression by Pb^{II} in the C110S and C111S mutants, compared to wild-type $CmtR^{Sc}$, whereas Cd^{II} responsiveness is substantially reduced. These results, when considered in the context of the metal binding properties of wild-type and C110G/C111S $CmtR^{Sc}$, reveal that coordination to metal site 2 in $CmtR^{Sc}$ is required for full transcriptional derepression by Cd^{II} in the cell. In contrast, Pb^{II} is a less potent inducer of *cmt-lacZ* expression *in vivo* and does not require metal site 2 for this activity.

DISCUSSION

$CmtR^{Sc}$ (SCO0875) is a *M. tuberculosis* CmtR homologue in *S. coelicolor* that shares 52% sequence identity with $CmtR^{Mtb}$.

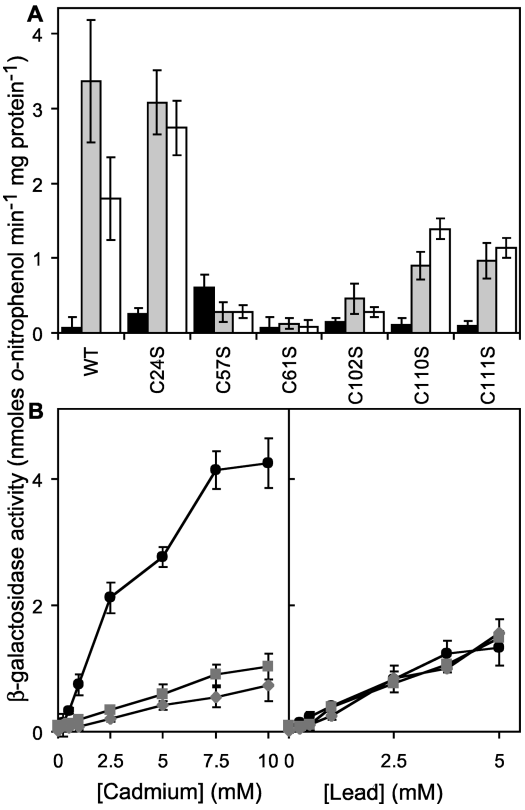

FIGURE 7: Metal-sensing ligands of $CmtR^{Sc}$. (A) β-Galactosidase activity measured in *M. smegmatis* mc^2155 containing wild-type $CmtR^{Sc}$ (WT) or derivatives with indicated cysteine to serine codon substitutions, following growth in LB medium with no metal supplement (black) or maximum permissive concentrations of Cd^{II} (gray) or Pb^{II} (white). (B) β-Galactosidase activity in cells containing wild-type $CmtR^{Sc}$ (black circles) or the C110S (gray squares) and C111S derivatives (gray diamonds) grown in LB with up to inhibitory concentrations of Cd^{II} or Pb^{II}. Data points represent the mean (±SE) for three independent experiments, each performed in triplicate.

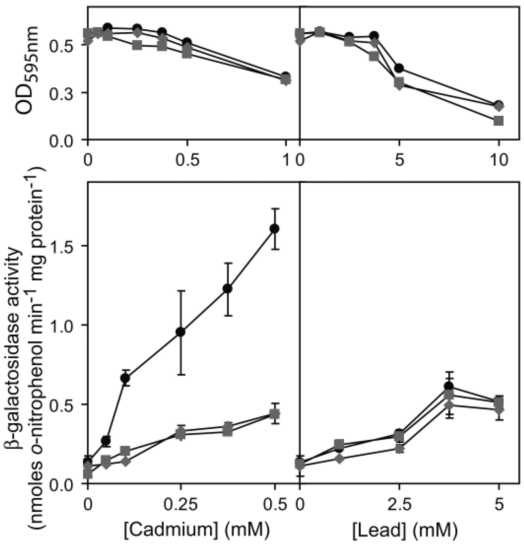

FIGURE 8: Metal-sensing ligands of $CmtR^{Sc}$ as determined on a chemically defined minimal medium. Top panel: Cell viability of *M. smegmatis* mc^2155 containing wild-type $CmtR^{Sc}$ (black circles) and C110S (gray squares) and C111S derivatives (gray diamonds) grown on minimal Sauton medium (containing 2.9 mM phosphate) as a function of total added Cd^{II} (left) or Pb^{II} (right). Lower panel: β-Galactosidase activity in cells containing wild-type $CmtR^{Sc}$ (black circles) and C110S (gray squares) or C111S $CmtR^{Sc}$ (gray diamonds) grown in minimal media up to inhibitory concentrations of Cd^{II} or Pb^{II}. Data points represent the mean (±SE) for three independent experiments, each performed in triplicate.

S. coelicolor belongs to the same taxonomic order (Actinomycetales) as the causative agents of tuberculosis and leprosy (*M. tuberculosis and Mycobacterium leprae*) but is a soil-dwelling bacterium that may more often encounter heavy metal polluted environments (*14*). However, *M. tuberculosis* is also suggested to encounter heavy metal ions such as Cd^{II} due to their accumulation in alveolar macrophages as a result of air pollution and cigarette smoking (*9*). As a result, metal-specific regulatory machinery is required to manage the intracellular concentrations of these ions (*1*). *M. tuberculosis* CmtR is the founding member of a subfamily of winged helical DNA binding repressors from the ArsR metal-sensing family that employ characteristic α4C metal sites that respond selectively to Cd^{II} and Pb^{II} (*6*−*8*). A search of $CmtR^{Mtb}$ homologues in *S. coelicolor* identified two nearly identical open reading frames (locus tags SCO0875 and SCO3522) that appear to encode a $CmtR^{Sc}$ that differ by just ten amino acids and immediately upstream of ORFs that encode what are predicted to be nearly identical cation diffusion facilitator (CDF) family heavy metal transporters. The presence of what would appear to be two functionally redundant operons may well reflect the need for *S. coelicolor* to rapidly sense and efflux (or otherwise detoxify) any Cd^{II} and Pb^{II} encountered in the environment.

In this study, we chose the gene encoded by locus tag SCO0875 as representative of $CmtR^{Sc}$ for detailed study and comparison with $CmtR^{Mtb}$. We were particularly intrigued by the presence of two C-terminal vicinal cysteines in $CmtR^{Sc}$, Cys110 and Cys111, both of which are conserved in SCO0875 and SCO3522. Substitution of these residues with nonliganding residues was expected to yield a regulator that behaves much like wild-type $CmtR^{Mtb}$. *In vitro* metal titration experiments confirm this but also reveal a second metal site in $CmtR^{Sc}$ which is formed by Cys-S^- coordination bonds donated by Cys110, Cys111, and a third as yet unidentified ligand. Cys24, which is at least partly exposed to solvent in the solution structure of Cd^{II}-bound CmtR (Figure 1B) (*8*) could readily complete an S_3 or $S_3(O)$ coordination complex. Since the solution structural model of Cd^{II}-bound CmtR ends at Arg106, this suggests that the C-terminal tail is highly flexible; if so, inspection of this structure suggests that the C-terminal Cys110/Cys111 pair of one subunit could potentially come in close physical proximity of Cys24 in the α2 helix of the same subunit by crossing over the "front" of the molecule in the orientation shown in Figure 1B. In this case, however, Cys24 *cannot* function as a key regulatory residue since *in vivo* β-galactosidase assays reveal that substitution of Cys24 does not influence Cd^{II} responsiveness of $CmtR^{Sc}$ in contrast to Cys110 and Cys111; a similar finding characterizes the primary α4C metal site in C24S $CmtR^{Mtb}$ (*6*). Cys24 may still complete the coordination structure of metal site 2, but it may simply increase the affinity of the site for Cd^{II} rather than function as an allosteric residue (*23*), much like that found previously for His100 in the Zn^{II} sensor *S. aureus* CzrA (*42*) and the Cys7 and Cys58 of the S_4 Cd^{II} sensor *S. aureus* pI258 CadC (*12*). Other nonthiolate possibilities for the third ligand are of course formally possible but would not be compatible with the absorption spectroscopy of the Cd^{II} and Pb^{II} complexes (*12*). Detailed structural or ^{113}Cd NMR studies (*7*, *12*, *32*) will be required to further elucidate the coordination structure of metal site 2 in $CmtR^{Sc}$.

$CmtR^{Sc}$ displays an *in vivo* metal specificity for Cd^{II} and Pb^{II} that is identical to that of $CmtR^{Mtb}$ in the heterologous host

M. smegmatis; given the similarity of these two bacterial species, these findings suggest that $CmtR^{Sc}$ is a *bona fide* Cd^{II}/Pb^{II} sensor in *S. coelicolor*. Although both $CmtR^{Sc}$ and $CmtR^{Mtb}$ share the same primary allosteric α4C metal site with the Hg^{II} sensor MerR in *Streptomyces lividans* (*43*), neither CmtR senses Hg^{II} in *M. smegmatis* (*7*). In addition, neither $CmtR^{Sc}$- nor $CmtR^{Mtb}$-repressed transcription is inducible by Zn^{II} (*7*), despite the fact that each retains the ability to bind Zn^{II} *in vitro* (*7*). Little is known about how *Streptomyces* spp. handle Hg^{II} toxicity and how this might differ from *Mycobacteria*; as a result, it is formally possible that, in addition to detecting Cd^{II} and Pb^{II}, $CmtR^{Sc}$ may detect Hg^{II} in the native host. A more important issue is how CmtRs sense Cd^{II} and Pb^{II} over Zn^{II} in the cell. Although absolute metal affinity of the sensing sites may not fully explain metal selectivity in the cell, this simple explanation may be at least partially operative here. Both proteins have Zn^{II} affinity $\leq 10^{10}$ M^{-1}, which is 3 orders less than the affinity for Cd^{II} (Figure 3) (*7*) which itself is comparable to that previously measured K_{Cd} for the Cd^{II}/Pb^{II} sensor CadC (*27*). Furthermore, a $K_{Zn} \leq 10^{10}$ M^{-1} may not be sufficient to be detected in cells by CmtR, since the typical bacterial Zn^{II} sensor is characterized by an equilibrium affinity for Zn^{II} in the 10^{12} to 10^{15} M^{-1} range. In fact, a protein encoded by locus tag SCO6459 is a strong candidate α5 site zinc sensor in *S. coelicolor* that may be poised to detect weakly chelated Zn^{II} buffered in the 10^{-12} to 10^{-15} M range (*29*, *42*, *44*, *45*). This ensures that both *cmtR*^{Sc}*-sco0874* and *sco3522-sco3521* operons will be induced by Cd^{II} and Pb^{II} and not by Zn^{II} so that these toxic metals can be selectively effluxed from the cytosol.

The primary α4C metal site 1 is necessary for both Cd^{II} and Pb^{II} detection in the cell but is not sufficient for full Cd^{II} responsiveness, which clearly requires coordination by metal site 2 (Figures 7 and 8). The evolutionary advantage of this to *S. coelicolor* is unknown but may reflect the possibility that Cd^{II} salts and low molecular weight complexes are far more bioavailable (soluble) in soils than Pb^{II} complexes (which may be readily precipitated) and thus must be more efficiently detoxified. Clearly, Cd^{II} is a stronger inducer of $CmtR^{Sc}$-mediated transcriptional derepression in *M. smegmatis* than is Pb^{II} over a similar concentration range of added metal, and most of this difference can be traced to Cd^{II} occupancy of metal site 2 (Figures 6 and 7). Pb^{II}, being the larger cation, may well fail to induce the same change in homodimer structure and/or dynamics that has been shown to be important in $CmtR^{Mtb}$ (*8*) and other ArsR family sensors (*46*). Alternatively, the bioavailable concentration of Pb^{II} achievable in *M. smegmatis* at the maximum permissive concentration of this cation (≈5 mM; Figures 7 and 8) may not be high enough to fill metal site 2 in the *M. smegmatis* cytosol; as a result, $CmtR^{Sc}$ is a poorer Pb^{II} sensor *in vivo*. In any case, filling both metal sites in $CmtR^{Sc}$ may well stabilize the allosterically inhibited low-affinity DNA binding state beyond that which can be achieved by filling the pair of primary α4C metal sites alone. Indeed, previous quantitative DNA binding experiments reveal that Cd^{II} is a relative poorer allosteric negative inhibitor of $CmtR^{Mtb}$ binding to DNA relative to other ArsR family metalloregulatory proteins (*1*, *11*); this suggests that Cd^{II} binding to metal site 2 may further enhance allosteric regulation of DNA binding in a way that leads to increased transcription derepression in the cell. Alternatively or in addition, the second high-affinity ($K_{Cd} \geq 10^{12}$ M^{-1}) cadmium binding site on $CmtR^{Sc}$ may also simply allow *S. coelicolor* to sequester (chelate) more Cd^{II} under conditions of Cd^{II} stress once $CmtR^{Sc}$ is dissociated from its DNA operator. Understanding the structural and physiological role of metal site 2 in $CmtR^{Sc}$ requires further investigation.

$CmtR^{Sc}$ is not the first ArsR family regulator with two structurally distinct pairs of metalloregulatory sites per dimer. Other examples include the Cd^{II}/Pb^{II} sensor pI258 CadC (*12*) and Cu^{I} sensor *Oscillatoria brevis* BxmR (*11*). CadC employs four conserved Cys in Cd^{II}, Co^{II}, and Bi^{III} binding while adopting an S_3 coordination complex with Pb^{II} in its primary α3N metal site; Zn^{II} binding to a pair of C-terminal interhelical α5 sites is functionally silent in CadCs, while other CadCs and α3N-type sensors have dispensed with this site entirely (*12*, *47*). In BxmR, the α3N site is a major sensing site for Cd^{II} and Cu^{I}, the latter of which forms a binuclear $Cu^{I}_2S_4$ cluster (*11*); a C-terminal α5 site has evolved exclusively for Zn^{II} sensing. Thus, in the case of BxmR, the presence of two distinct metal sites relaxes the metal selectivity of this particular sensor. In $CmtR^{Sc}$, the impact of metal site 2 on $CmtR^{Sc}$ function largely parallels the situation in CadCs, where the secondary site does not change the metal specificity profile of the primary metal site (*12*, *48*) but, unlike in CadCs, enhances its effectiveness in the cell.

Finally, $CmtR^{Sc}$ is the first ArsR family metal sensor to be characterized from *S. coelicolor* and is shown here to possess both a metal-sensing site anticipated on the basis of its classification as an CmtR-like α4C Pb^{II}/Cd^{II} sensor, as well as a second novel metalloregulatory site not found in other CmtRs. In fact, the presence of consecutive or vicinal Cys residues in what are predicted to be flexible or unstructured N-terminal or C-terminal "tails" like that in metal site 2 in $CmtR^{Sc}$ has previously been shown to function as As^{III} ligands in two arsenic-specific ArsR family proteins recently characterized (*49*, *50*); given this, it seemed possible that Cys110 and/or Cys111 might confer an As^{III}-sensing function on the Pb^{II}/Cd^{II}-sensing CmtR. Our data reveal that this is not the case, at least as measured by transcriptional derepression in *M. smegmatis* (Figure 6). These findings are consistent with the idea that ArsR family sensors may well be readily classified into subfamilies of paralogues that detect distinct cellular inducers solely on the basis of well-characterized primary structural motifs, rather than global sequence similarity (*1*, *10*). However, these core characteristics can be modulated by additional or altogether novel metal sites capable of tuning inducer responsiveness appropriate for the microenvironmental niche in which an organism resides (*11*, *49*).

REFERENCES

1. Ma, Z., Jacobsen, F. E., and Giedroc, D. P. (2009) Coordination chemistry of bacterial metal transport and sensing. *Chem. Rev. 109*, 4644–4681.
2. Nies, D. H. (2000) Heavy metal-resistant bacteria as extremophiles: molecular physiology and biotechnological use of *Ralstonia* sp. CH34. *Extremophiles 4*, 77–82.
3. Schnappinger, D., Ehrt, S., Voskuil, M. I., Liu, Y., Mangan, J. A., Monahan, I. M., Dolganov, G., Efron, B., Butcher, P. D., Nathan, C., and Schoolnik, G. K. (2003) Transcriptional adaptation of *Mycobacterium tuberculosis* within macrophages: insights into the phagosomal environment. *J. Exp. Med. 198*, 693–704.
4. Payne, J. C., ter Horst, M. A., and Godwin, H. A. (1999) Lead fingers: Pb^{2+} binding to structural zinc-binding domains determined directly by monitoring lead-thiolate charge-transfer bands. *J. Am. Chem. Soc. 121*, 6850–6855.
5. Warren, M. J., Cooper, J. B., Wood, S. P., and Shoolingin-Jordan, P. M. (1998) Lead poisoning, haem synthesis and 5-aminolaevulinic acid dehydratase. *Trends Biochem. Sci. 23*, 217–221.
6. Cavet, J. S., Graham, A. I., Meng, W., and Robinson, N. J. (2003) A cadmium-lead-sensing ArsR-SmtB repressor with novel sensory sites. Complementary metal discrimination by NmtR and CmtR in a common cytosol. *J. Biol. Chem. 278*, 44560–44566.

7. Wang, Y., Hemmingsen, L., and Giedroc, D. P. (2005) Structural and functional characterization of *Mycobacterium tuberculosis* CmtR, a PbII/CdII-sensing SmtB/ArsR metalloregulatory repressor. *Biochemistry 44*, 8976–8988.
8. Banci, L., Bertini, I., Cantini, F., Ciofi-Baffoni, S., Cavet, J. S., Dennison, C., Graham, A. I., Harvie, D. R., and Robinson, N. J. (2007) NMR structural analysis of cadmium sensing by winged helix repressor CmtR. *J. Biol. Chem. 282*, 30181–30188.
9. Chauhan, S., Kumar, A., Singhal, A., Tyagi, J. S., and Krishna Prasad, H. (2009) CmtR, a cadmium-sensing ArsR-SmtB repressor, cooperatively interacts with multiple operator sites to autorepress its transcription in *Mycobacterium tuberculosis*. *FEBS J. 276*, 3428–3439.
10. Campbell, D. R., Chapman, K. E., Waldron, K. J., Tottey, S., Kendall, S., Cavallaro, G., Andreini, C., Hinds, J., Stoker, N. G., Robinson, N. J., and Cavet, J. S. (2007) Mycobacterial cells have dual nickel-cobalt sensors: sequence relationships and metal sites of metal-responsive repressors are not congruent. *J. Biol. Chem. 282*, 32298–32310.
11. Liu, T., Chen, X., Ma, Z., Shokes, J., Hemmingsen, L., Scott, R. A., and Giedroc, D. P. (2008) A Cu(I)-sensing ArsR family metal sensor protein with a relaxed metal selectivity profile. *Biochemistry 47*, 10564–10575.
12. Busenlehner, L. S., Weng, T. C., Penner-Hahn, J. E., and Giedroc, D. P. (2002) Elucidation of primary (α3N) and vestigial (α5) heavy metal-binding sites in *Staphylococcus aureus* pI258 CadC: evolutionary implications for metal ion selectivity of ArsR/SmtB metal sensor proteins. *J. Mol. Biol. 319*, 685–701.
13. Ye, J., Kandegedara, A., Martin, P., and Rosen, B. P. (2005) Crystal structure of the *Staphylococcus aureus* pI258 CadC Cd(II)/Pb(II)/Zn(II)-responsive repressor. *J. Bacteriol. 187*, 4214–4221.
14. Bentley, S. D., Chater, K. F., Cerdeno-Tarraga, A. M., Challis, G. L., Thomson, N. R., James, K. D., Harris, D. E., Quail, M. A., Kieser, H., Harper, D., Bateman, A., Brown, S., Chandra, G., Chen, C. W., Collins, M., Cronin, A., Fraser, A., Goble, A., Hidalgo, J., Hornsby, T., Howarth, S., Huang, C. H., Kieser, T., Larke, L., Murphy, L., Oliver, K., O'Neil, S., Rabbinowitsch, E., Rajandream, M. A., Rutherford, K., Rutter, S., Seeger, K., Saunders, D., Sharp, S., Squares, R., Squares, S., Taylor, K., Warren, T., Wietzorrek, A., Woodward, J., Barrell, B. G., Parkhill, J., and Hopwood, D. A. (2002) Complete genome sequence of the model actinomycete *Streptomyces coelicolor* A3(2). *Nature 417*, 141–147.
15. Borodina, I., Krabben, P., and Nielsen, J. (2005) Genome-scale analysis of *Streptomyces coelicolor* A3(2) metabolism. *Genome Res. 15*, 820–829.
16. Wagner, D., Maser, J., Lai, B., Cai, Z., Barry, C. E., III, Honer Zu Bentrup, K., Russell, D. G., and Bermudez, L. E. (2005) Elemental analysis of *Mycobacterium avium*-, *Mycobacterium tuberculosis*-, and *Mycobacterium smegmatis*-containing phagosomes indicates pathogen-induced microenvironments within the host cell's endosomal system. *J. Immunol. 174*, 1491–1500.
17. Collins, H. L. (2008) Withholding iron as a cellular defence mechanism—friend or foe? *Eur. J. Immunol. 38*, 1803–1806.
18. White, C., Lee, J., Kambe, T., Fritsche, K., and Petris, M. J. (2009) A role for the ATP7A copper-transporting ATPase in macrophage bactericidal activity. *J. Biol. Chem. 284*, 33949–33956.
19. Techau, M. E., Valdez-Taubas, J., Popoff, J. F., Francis, R., Seaman, M., and Blackwell, J. M. (2007) Evolution of differences in transport function in Slc11a family members. *J. Biol. Chem. 282*, 35646–35656.
20. An, Y. J., Ahn, B. E., Han, A. R., Kim, H. M., Chung, K. M., Shin, J. H., Cho, Y. B., Roe, J. H., and Cha, S. S. (2009) Structural basis for the specialization of Nur, a nickel-specific Fur homolog, in metal sensing and DNA recognition. *Nucleic Acids Res.* 3442–3451.
21. Ahn, B. E., Cha, J., Lee, E. J., Han, A. R., Thompson, C. J., and Roe, J. H. (2006) Nur, a nickel-responsive regulator of the Fur family, regulates superoxide dismutases and nickel transport in *Streptomyces coelicolor*. *Mol. Microbiol. 59*, 1848–1858.
22. Shin, J. H., Oh, S. Y., Kim, S. J., and Roe, J. H. (2007) The zinc-responsive regulator Zur controls a zinc uptake system and some ribosomal proteins in *Streptomyces coelicolor* A3(2). *J. Bacteriol. 189*, 4070–4077.
23. Giedroc, D. P., and Arunkumar, A. I. (2007) Metal sensor proteins: nature's metalloregulated allosteric switches. *Dalton Trans. 29*, 3107–3120.
24. Montanini, B., Blaudez, D., Jeandroz, S., Sanders, D., and Chalot, M. (2007) Phylogenetic and functional analysis of the cation diffusion facilitator (CDF) family: improved signature and prediction of substrate specificity. *BMC Genomics 8*, 107.
25. Guo, J., and Giedroc, D. P. (1997) Zinc site redesign in T4 gene 32 protein: structure and stability of cobalt(II) complexes formed by wild-type and metal ligand substitution mutants. *Biochemistry 36*, 730–742.
26. Tan, X., Kagiampakis, I., Surovtsev, I. V., Demeler, B., and Lindahl, P. A. (2007) Nickel-dependent oligomerization of the alpha subunit of acetyl-coenzyme a synthase/carbon monoxide dehydrogenase. *Biochemistry 46*, 11606–11613.
27. Busenlehner, L. S., Cosper, N. J., Scott, R. A., Rosen, B. P., Wong, M. D., and Giedroc, D. P. (2001) Spectroscopic properties of the metalloregulatory Cd(II) and Pb(II) sites of *S. aureus* pI258 CadC. *Biochemistry 40*, 4426–4436.
28. Martell, A. E., and Smith, R. M. (1979−1989) Critical Stability Constants, Plenum Press, New York.
29. VanZile, M. L., Chen, X., and Giedroc, D. P. (2002) Structural characterization of distinct α3N and α5 metal sites in the cyanobacterial zinc sensor SmtB. *Biochemistry 41*, 9765–9775.
30. Timm, J., Lim, E. M., and Gicquel, B. (1994) *Escherichia coli*-mycobacteria shuttle vectors for operon and gene fusions to lacZ: the pJEM series. *J. Bacteriol. 176*, 6749–6753.
31. Cavet, J. S., Meng, W., Pennella, M. A., Appelhoff, R. J., Giedroc, D. P., and Robinson, N. J. (2002) A nickel-cobalt-sensing ArsR-SmtB family repressor. Contributions of cytosol and effector binding sites to metal selectivity. *J. Biol. Chem. 277*, 38441–38448.
32. Matzapetakis, M., Farrer, B. T., Weng, T. C., Hemmingsen, L., Penner-Hahn, J. E., and Pecoraro, V. L. (2002) Comparison of the binding of cadmium(II), mercury(II), and arsenic(III) to the de novo designed peptides TRI L12C and TRI L16C. *J. Am. Chem. Soc. 124*, 8042–8054.
33. Pountney, D. L., Tiwari, R. P., and Egan, J. B. (1997) Metal- and DNA-binding properties and mutational analysis of the transcription activating factor, B, of coliphage 186: a prokaryotic C4 zinc-finger protein. *Protein Sci. 6*, 892–902.
34. Henehan, C. J., Pountney, D. L., Zerbe, O., and Vasak, M. (1993) Identification of cysteine ligands in metalloproteins using optical and NMR spectroscopy: cadmium-substituted rubredoxin as a model $[Cd(CysS)4]^{2-}$ center. *Protein Sci. 2*, 1756–1764.
35. Claudio, E. S., Magyar, J. S., and Godwin, H. A. (2003) *Prog. Inorg. Chem. 51*, 1–144.
36. Magyar, J. S., Weng, T. C., Stern, C. M., Dye, D. F., Rous, B. W., Payne, J. C., Bridgewater, B. M., Mijovilovich, A., Parkin, G., Zaleski, J. M., Penner-Hahn, J. E., and Godwin, H. A. (2005) Reexamination of lead(II) coordination preferences in sulfur-rich sites: implications for a critical mechanism of lead poisoning. *J. Am. Chem. Soc. 127*, 9495–9505.
37. Gamelin, D. R., Randall, D. W., Hay, M. T., Houser, R. P., Mulder, T. C., Canters, G. W., de Vries, S., Tolman, W. B., Lu, Y., and Solomon, E. I. (1998) Spectroscopy of mixed-valence CuA-type centers: ligand-field control of ground-state properties related to electron transfer. *J. Am. Chem. Soc. 120*, 5246–5263.
38. Basumallick, L., George, S. D., Randall, D. W., Hedman, B., Hodgson, K. O., Fujisawa, K., and Solomon, E. I. (2002) Spectroscopic comparison of the five-coordinate [Cu(SMeIm)(HB(3,5-iPr2pz)$_3$)] with the four-coordinate [Cu(SCPh3)(HB(3,5-iPr2pz)$_3$)]: effect of coordination number increase on a blue copper type site. *Inorg. Chim. Acta 337*, 357–365.
39. Lever, A. B. P. (1974) *J. Chem. Educ. 51*, 612–616.
40. Hernandez-Abanto, S. M., Woolwine, S. C., Jain, S. K., and Bishai, W. R. (2006) Tetracycline-inducible gene expression in mycobacteria within an animal host using modified *Streptomyces* tcp830 regulatory elements. *Arch. Microbiol. 186*, 459–464.
41. Raghunand, T. R., and Bishai, W. R. (2006) Mapping essential domains of *Mycobacterium smegmatis* WhmD: insights into WhiB structure and function. *J. Bacteriol. 188*, 6966–6976.
42. Pennella, M. A., Arunkumar, A. I., and Giedroc, D. P. (2006) Individual metal ligands play distinct functional roles in the zinc sensor *Staphylococcus aureus* CzrA. *J. Mol. Biol. 356*, 1124–1136.
43. Rother, D., Mattes, R., and Altenbuchner, J. (1999) Purification and characterization of MerR, the regulator of the broad-spectrum mercury resistance genes in *Streptomyces lividans* 1326. *Mol. Gen. Genet. 262*, 154–162.
44. Outten, C. E., and O'Halloran, T. V. (2001) Femtomolar sensitivity of metalloregulatory proteins controlling zinc homeostasis. *Science 292*, 2488–2492.
45. Waldron, K. J., and Robinson, N. J. (2009) How do bacterial cells ensure that metalloproteins get the correct metal? *Nat. Rev. Microbiol. 7*, 25–35.
46. Arunkumar, A. I., Campanello, G. C., and Giedroc, D. P. (2009) Solution structure of a paradigm ArsR family zinc sensor in the DNA-bound state. *Proc. Natl. Acad. Sci. U.S.A. 106*, 18177–18182.

47. Liu, T., Golden, J. W., and Giedroc, D. P. (2005) A zinc(II)/lead(II)/cadmium(II)-inducible operon from the cyanobacterium *Anabaena* is regulated by AztR, an α3N ArsR/SmtB metalloregulator. *Biochemistry 44*, 8673–8683.
48. Kandegedara, A., Thiyagarajan, S., Kondapalli, K. C., Stemmler, T. L., and Rosen, B. P. (2009) Role of bound Zn(II) in the CadC Cd(II)/Pb(II)/Zn(II)-responsive repressor. *J. Biol. Chem. 284*, 14958–14965.
49. Ordoñez, E., Thiyagarajan, S., Cook, J. D., Stemmler, T. L., Gil, J. A., Mateos, L. M., and Rosen, B. P. (2008) Evolution of metal(loid) binding sites in transcriptional regulators. *J. Biol. Chem. 283*, 25706–25714.
50. Qin, J., Fu, H. L., Ye, J., Bencze, K. Z., Stemmler, T. L., Rawlings, D. E., and Rosen, B. P. (2007) Convergent evolution of a new arsenic binding site in the ArsR/SmtB family of metalloregulators. *J. Biol. Chem. 282*, 34346–34355.